

HEP Theory

Costas Papadopoulos

Friday, May 6, 2023

Group Structure and Personnel

- C. Papadopoulos

- D. Canko (PhD student)
- N. Syrrakos (PhD student)
- G. Bevilacqua, A. Kardos, M. Worek, A. van Hameren, M. Czakon, C. Duhr, J. Henn, S. Badger
- N. Tsolis (MSc-Thesis Student), V. Tzotzai (Diploma-Thesis Student)

- M. Axenides

- G. Linardopoulos
- G. Pastras, I. Mitsoulas, D. Manolopoulos
- D. Katsinis (Ph.D-Thesis Student)
- E. Floratos, S. Nicolis, A. Pavlidis
- Papagrigoriou (MSc-Thesis Student)

- G. Savvidy

- S. Konitopoulos
- K. Filippas
- K. Savvidy
- Narek Martirosyan, Hasmik Poghosyan and Hayk Poghosyan (PhD students).

3 Biggest Physics Discoveries Of The Decade

<https://www.forbes.com>

Higgs

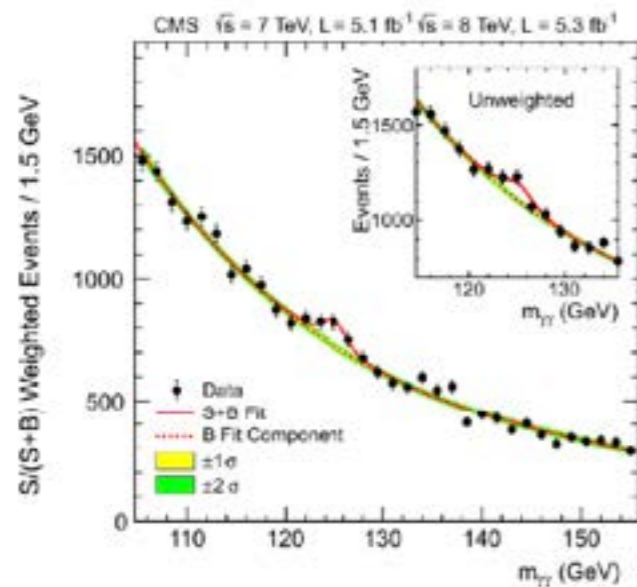


Fig. 3. The diphoton invariant mass distribution with each event weighted by the $S/(S+B)$ value of its category. The lines represent the fitted background and signal, and the coloured bands represent the ± 1 and ± 2 standard deviation uncertainties in the background estimate. The inset shows the central part of the unweighted invariant mass distribution. (For interpretation of the references to colour in this figure legend, the reader is referred to the web version of this Letter.)

GW

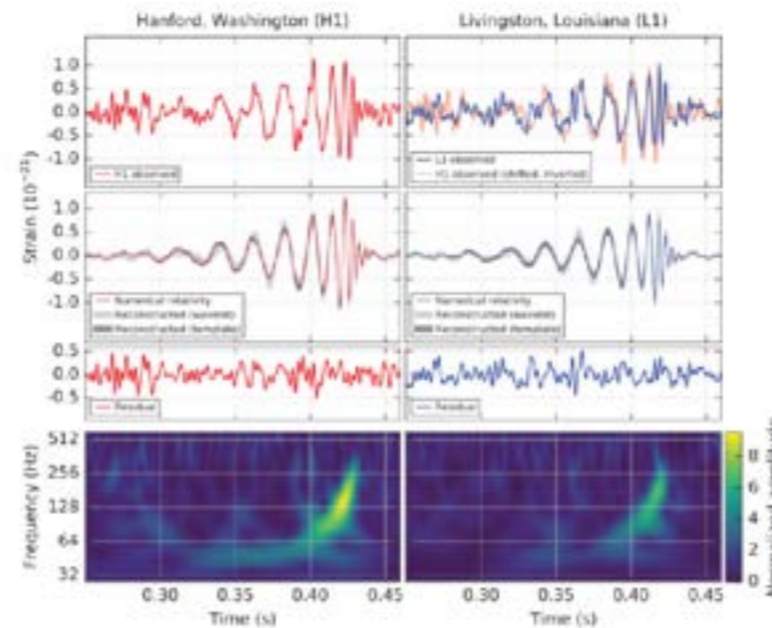


FIG. 4. The gravitational-wave event GW150914 observed by the LIGO Hanford (H1, left column panels) and Livingston (L1, right column panels) detectors. Times are shown relative to September 14, 2015 at 09:50:45 UTC. For visualization, all time series are filtered with a 35–350 Hz bandpass filter to suppress large fluctuations outside the detectors’ most sensitive frequency band, and band-pass filter to remove the strong instrumental spectral lines seen in the Fig. 3 spectra. Top row, left: H1 strain. Top row, right: L1 strain. GW150914 ambient data at L1 and 6.5–12.5 ms later at H1. (For a visual comparison, the H1 data are also shown, shifted in time by this amount and inverted [to account for the detectors’ relative orientations].) Second row: Characteristic-wave strain projected onto each detector in the 35–350 Hz band. Solid lines show a numerical relativity waveform for a system with parameters consistent with those measured from GW150914 [37,38] confirmed to 99.9% by an independent calculation based on [15]. Shaded areas show 90% credible regions for two independent waveform reconstructions. One (dark gray) models the signal using binary black hole template waveforms [39]. The other (light gray) does not use an astrophysical model, but instead calculates the strain signal as a linear combination of one-Gaussian wavelets [40,41]. These reconstructions have a 94% overlap, as shown in [39]. Third row: Results after subtracting the linear numerical relativity waveforms from the filtered detector time series. Bottom row: A time-frequency spectrogram [42] of the strain data, showing the signal frequency increasing over time.

BH Horizon

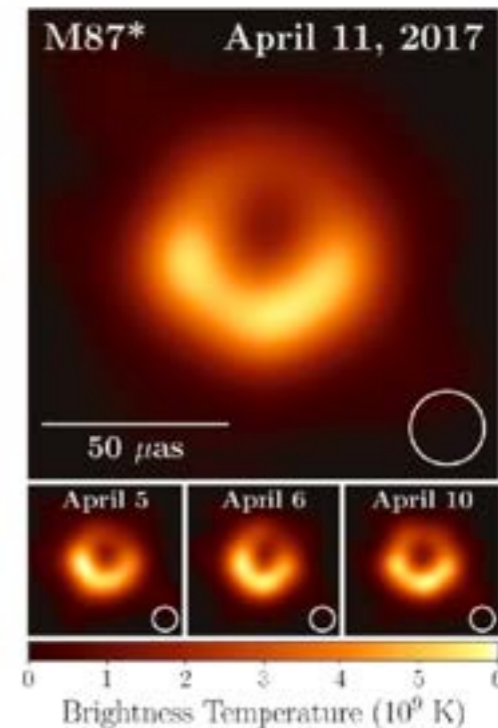
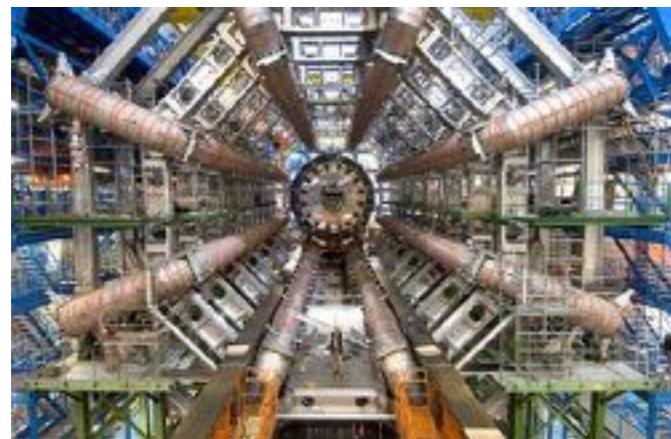


Figure 5. Top: EHT image of M87* from observations on 2017 April 11 as a representative example of the images collected in the 2017 campaign. The image is the average of three different imaging methods after convolving each with a circular Gaussian kernel to give matched resolutions. The largest of the three kernels (20 mas FWHM) is shown in the lower right. The image is shown in units of brightness temperature, $T_b = S\lambda^2/2k_B\Omega$, where S is the flux density, λ is the observing wavelength, k_B is the Boltzmann constant, and Ω is the solid angle of the resolution element. Bottom: similar images taken over different days showing the stability of the basic image structure and the equivalence among different days. North is up and east is to the left.

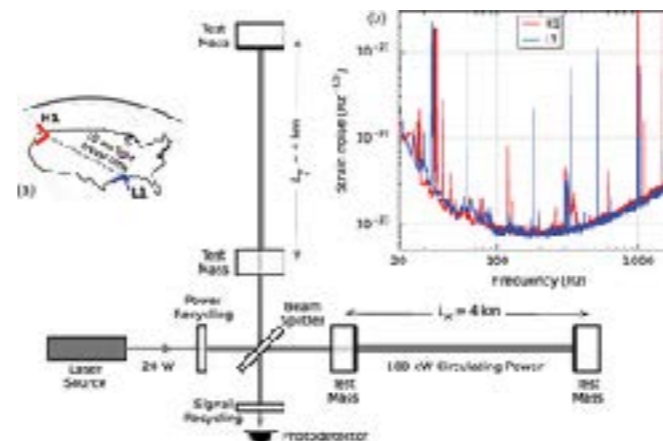
From elementary particles to Black Holes

LHC



ATLAS detector

LIGO



EHT

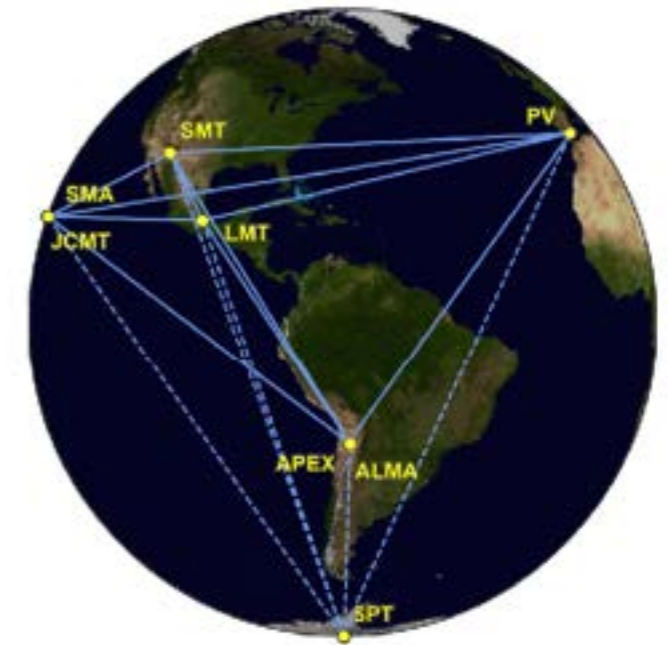


Figure 1. Eight stations of the EHT 2017 campaign over six geographic locations as viewed from the equatorial plane. Solid baselines represent mutual visibility on M87* ($+12^\circ$ declination). The dashed baselines were used for the calibration source 3C279 (see Papers III and IV).



Large Millimeter Telescope "Alfonso Serrano" (LMT)

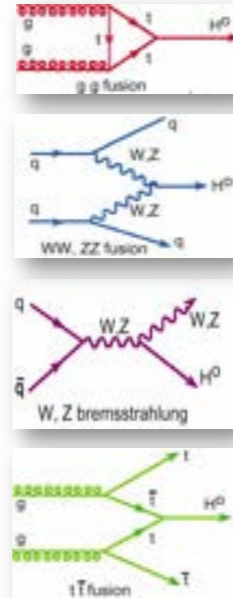
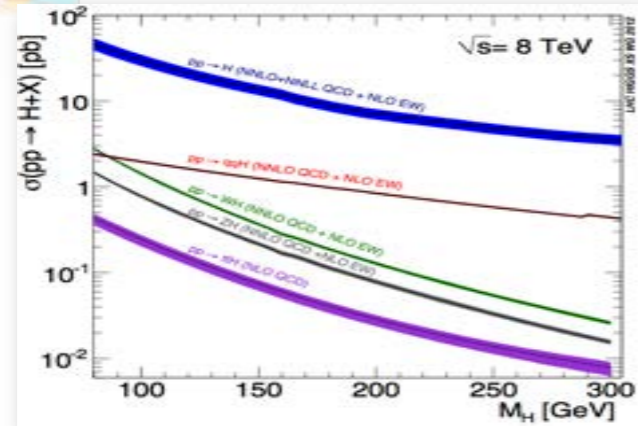
Theoretical Physics

QFT

Higgs boson production



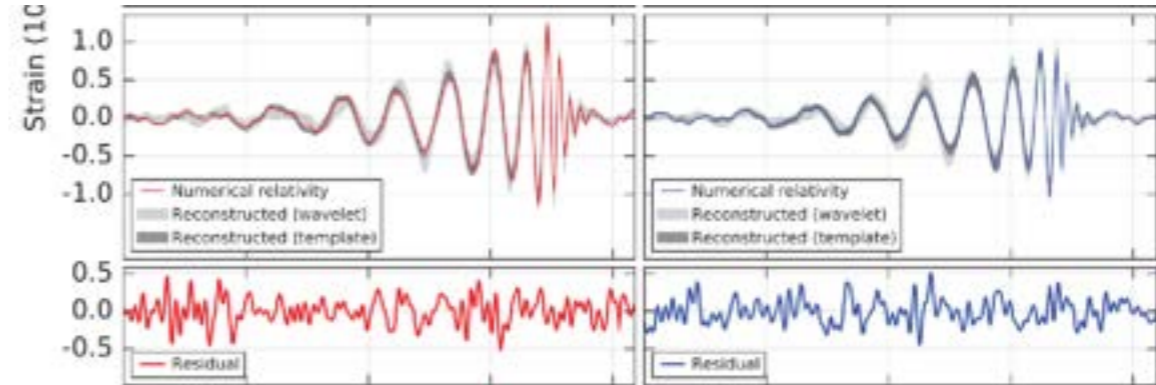
July 4th 2012 The Status of the Higgs Search J. Incandela for the CMS COLLABORATION



- $\sqrt{s}=8$ TeV: 25-30% higher σ than $\sqrt{s}=7$ TeV at low m_H
- All production modes to be exploited
 - gg VBF VH ttH
 - Latter 3 have smaller cross sections but better S/B in many cases

11

GR



BH Physics

Faint signals; Patience; Theory

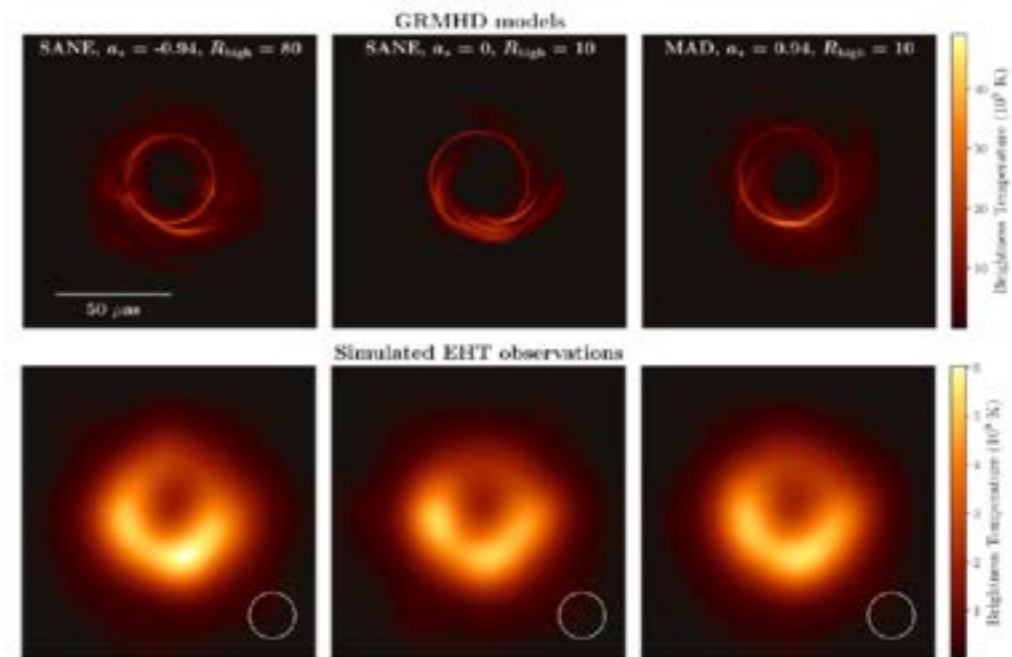
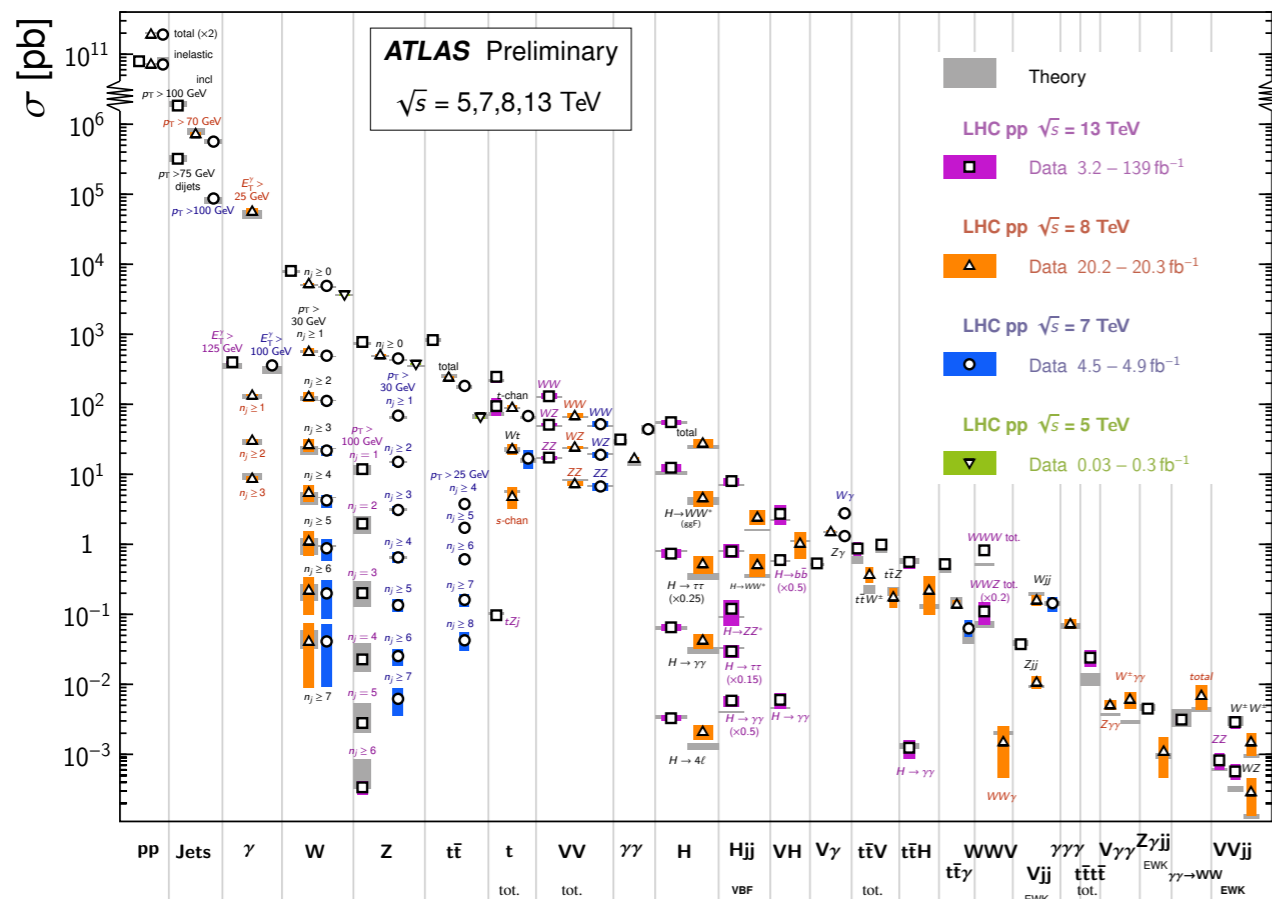


Figure 4. Top: three example models of some of the best-fitting snapshots from the image library of GRMHD simulations for April 11 corresponding to different spin parameters and accretion flows. Bottom: the same theoretical models, processed through a VLBI simulation pipeline with the same schedule, telescope characteristics, and weather parameters as in the April 11 run and imaged in the same way as Figure 3. Note that although the fit to the observations is equally good in the three cases, they refer to radically different physical accretions, this highlights that a single good fit does not imply that a model is preferred over others (see Paper V).

High Energy Physics Phenomenology and Computational Physics

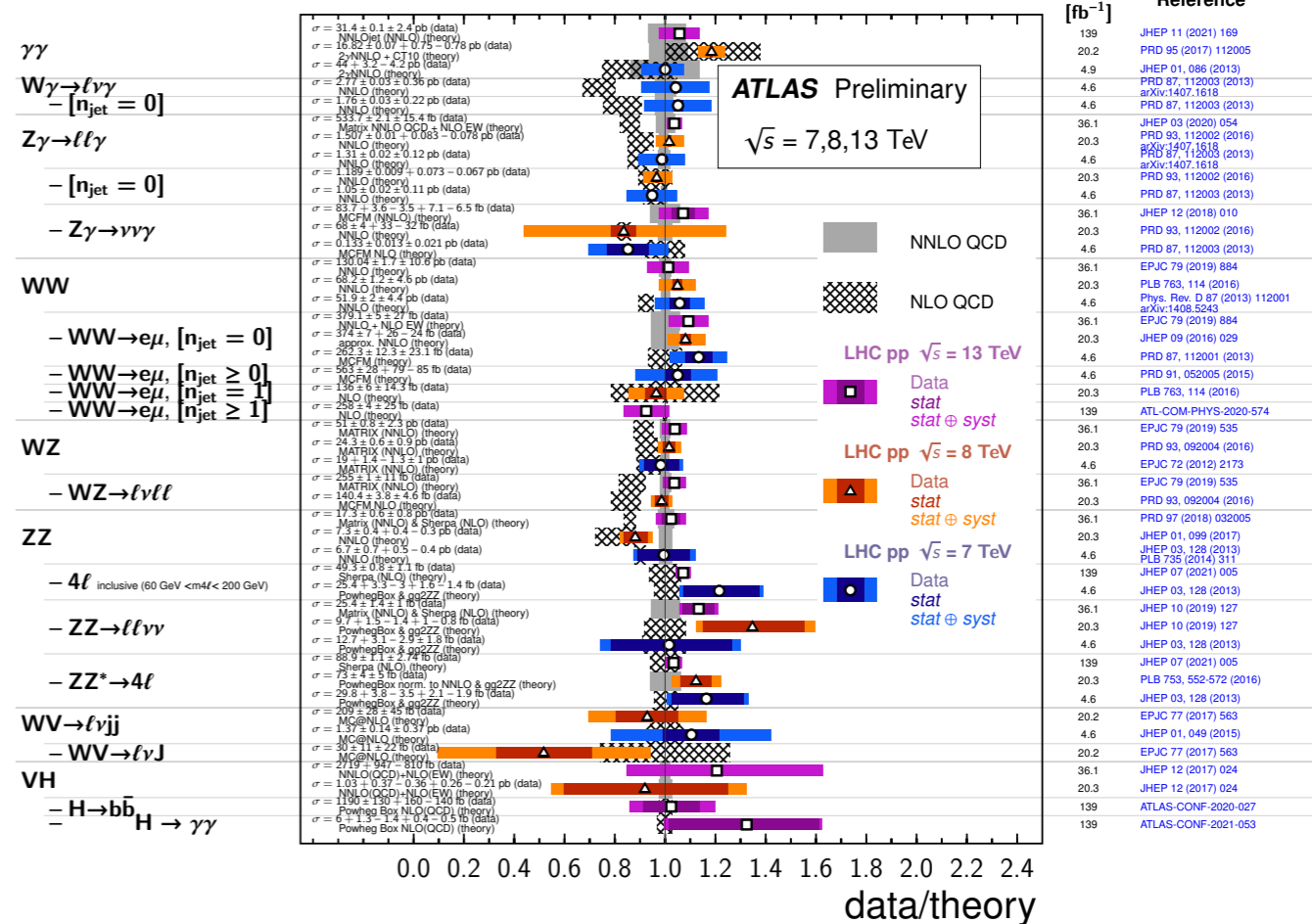
Standard Model Production Cross Section Measurements

Status: February 2022



Diboson Cross Section Measurements

Status: February 2022



Precision physics requires precise theoretical predictions

High Energy Physics Phenomenology and Computational Physics

Institute of Nuclear Physics "Demokritos" | Bergische Universität Wuppertal | Institute of Nuclear Physics PAN | RWTH Aachen University

HELAC-NLO & Associated Tools

[Projects](#) | [People](#) | [Contact us](#)

Projects

[HELAC-PHEGAS](#) - A generator for all parton level processes in the Standard Model
[HELAC-DIPOLES](#) - Dipole formalism for the arbitrary helicity eigenstates of the external partons
[HELAC-JLOOP](#) - A program for numerical evaluation of QCD virtual corrections to scattering amplitudes
[ONELOOP](#) - A program for the evaluation of one-loop scalar functions
[CUTTOOLS](#) - A program implementing the OPP reduction method to compute one-loop amplitudes
[FARNI](#) - A program for importance sampling and density estimation
[KALEU](#) - A general-purpose parton-level phase space generator
[HELAC-ONIA](#) - An automatic matrix element generator for heavy quarkonium physics

[:: top ::](#)

People

Giuseppe Bevilacqua
[Michał Czakon](#)
[Maria Vittoria Garzelli](#)
Andreas van Hameren
Adam Kardos
Yiannis Malamou
[Costas G. Papadopoulos](#)
[Roberto Pittau](#)
[Malgorzata Worek](#)
Hua-Sheng Shao

[:: top ::](#)

Contact us

If you have a question, comment, suggestion or bug report, please e-mail us at:

bevilacqua@physik.rwth-aachen.de
mczakon@physik.rwth-aachen.de
garzelli@to.infn.it
Andre.Hameren@ijf.edu.pl
kardam@t-online.hu
J.Malamas@science.ru.nl
Costas.Papadopoulos@cern.ch
pittau@lujr.es
Malgorzata.Worek@cern.ch
erdissshaw@gmail.com

[:: top ::](#)

Last modified by Malgorzata Worek
Thursday, January 10th, 2013

Proof of concept: the first NLO public code

One-loop Amplitudes

$$\mathcal{A} = \sum d_{i_1 i_2 i_3 i_4} \text{[square]} + \sum c_{i_1 i_2 i_3} \text{[triangle]} + \sum b_{i_1 i_2} \text{[circle]} + \sum a_{i_1} \text{[blob]} + R$$

$$\mathcal{A} = \sum_{I \subset \{0,1,\dots,m-1\}} \int \frac{\mu^{(4-d)d^d q}}{(2\pi)^d} \frac{\bar{N}_I(\bar{q})}{\prod_{i \in I} \bar{D}_i(\bar{q})}$$

OPP

$$N_I = \sum (d_{i_1 i_2 i_3 i_4} + \tilde{d}_{i_1 i_2 i_3 i_4}) D_{i_1} D_{i_2} D_{i_3} D_{i_4} + \sum (c_{i_1 i_2 i_3} + \tilde{c}_{i_1 i_2 i_3}) D_{i_1} D_{i_2} D_{i_3} + \dots$$

Nucl.Phys.B 763 (2007) 147-169

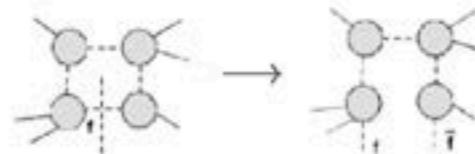
The computation of $pp(p\bar{p}) \rightarrow e^- \nu_e \mu^- \bar{\nu}_\mu b \bar{b}$ involves up to six-point functions. The most generic integrand has therefore the form

$$\mathcal{A}(q) = \sum \frac{N_i^{(6)}(q)}{\underbrace{\bar{D}_{i_0} \bar{D}_{i_1} \dots \bar{D}_{i_5}}_{\text{[6-point diagram]}}} + \frac{N_i^{(5)}(q)}{\underbrace{\bar{D}_{i_0} \bar{D}_{i_1} \dots \bar{D}_{i_4}}_{\text{[5-point diagram]}}} + \frac{N_i^{(4)}(q)}{\underbrace{\bar{D}_{i_0} \bar{D}_{i_1} \dots \bar{D}_{i_3}}_{\text{[4-point diagram]}}} + \frac{N_i^{(3)}(q)}{\underbrace{\bar{D}_{i_0} \bar{D}_{i_1} \bar{D}_{i_2}}_{\text{[3-point diagram]}}} + \dots$$

HELAC1L

In order to apply the OPP reduction, HELAC evaluates numerically the numerators $N_i^{(6)}(q), N_i^{(5)}(q), \dots$ with the values of the loop momentum q provided by CutTools

- generates all inequivalent partitions of 6,5,4,3... blobs attached to the loop, and check all possible flavours (and colours) that can be consistently running inside
- hard-cuts the loop (q is fixed) to get a $n + 2$ tree-like process



The R_2 contributions (rational terms) are calculated in the same way as the tree-order amplitude, taking into account *extra vertices*

High Energy Physics Phenomenology and Computational Physics

NNLO precision

$$\sigma_{NNLO} \rightarrow \int_m d\Phi_m \left(2 \operatorname{Re}(M_m^{(0)*} M_m^{(2)}) + |M_m^{(1)}|^2 \right) J_m(\Phi) \quad \mathbf{VV}$$

$$+ \int_{m+1} d\Phi_{m+1} \left(2 \operatorname{Re}(M_{m+1}^{(0)*} M_{m+1}^{(1)}) \right) J_{m+1}(\Phi) \quad \mathbf{RV}$$

$$+ \int_{m+2} d\Phi_{m+2} |M_{m+2}^{(0)}|^2 J_{m+2}(\Phi) \quad \mathbf{RR}$$

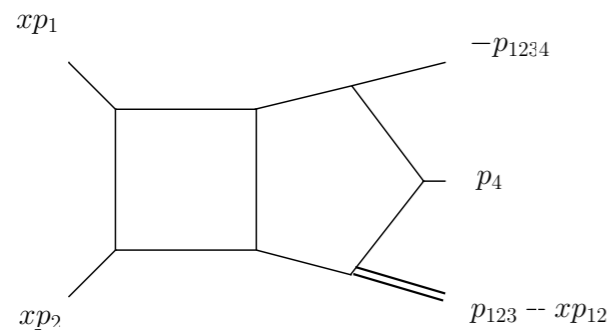
Renormalisation, Factorisation

Tree-order, one- and two-loop amplitudes

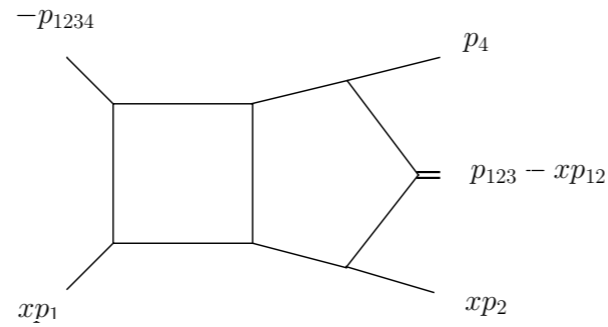
High Energy Physics Phenomenology and Computational Physics

Two-loop integrals: planar case

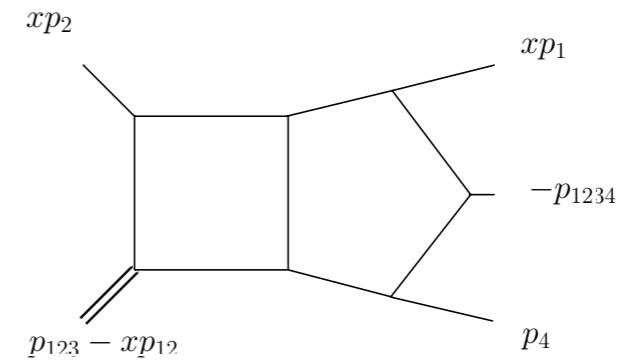
Feynman : September 15, 1949



74,3



75,3



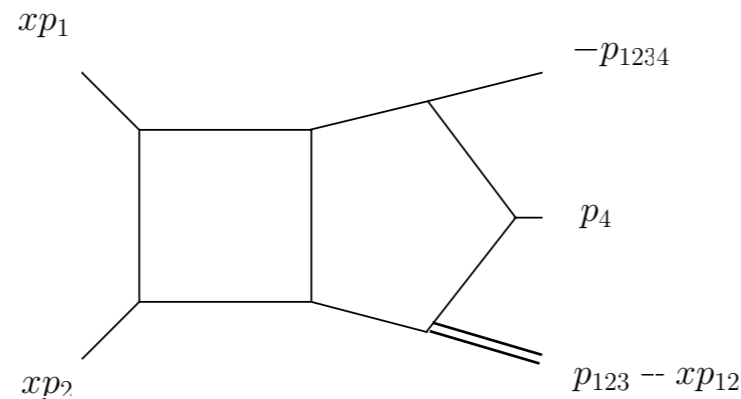
86,3

$$G_{a_1 \dots a_{11}}^{P_1} = e^{2\gamma_E \varepsilon} \int \frac{d^d k_1}{i\pi^{d/2}} \frac{d^d k_2}{i\pi^{d/2}} \frac{1}{k_1^{2a_1} (k_1 + q_1)^{2a_2} (k_1 + q_{12})^{2a_3} (k_1 + q_{123})^{2a_4} k_2^{2a_5} (k_2 + q_{123})^{2a_6} (k_2 + q_{1234})^{2a_7} (k_1 - k_2)^{2a_8} (k_1 + q_{1234})^{2a_9} (k_2 + q_1)^{2a_{10}} (k_2 + q_{12})^{2a_{11}}}$$

High Energy Physics Phenomenology and Computational Physics

Simplified Differential Equations

[JHEP 07 \(2014\), 088](#)



$$q_1 \rightarrow p_{123} - xp_{12}, q_2 \rightarrow p_4, q_3 \rightarrow -p_{1234}, q_4 \rightarrow xp_1$$

$$d\vec{g} = \epsilon \sum_a d \log(W_a) \tilde{M}_a \vec{g} \qquad \frac{d\vec{g}}{dx} = \epsilon \sum_b \frac{1}{x - \ell_b} M_b \vec{g}$$

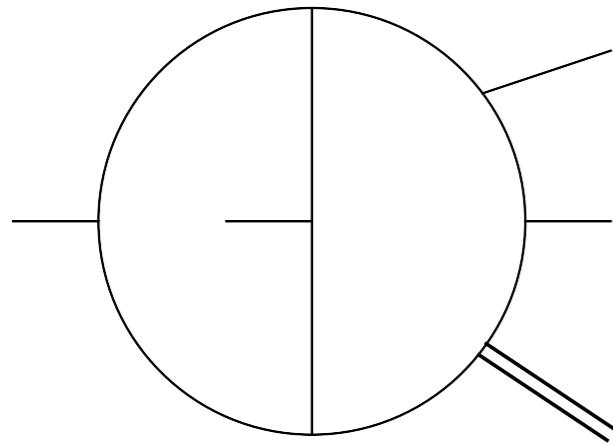
$$\begin{aligned} \vec{g} &= \epsilon^0 \mathbf{b}_0^{(0)} + \epsilon \left(\sum \mathcal{G}_a \mathbf{M}_a \mathbf{b}_0^{(0)} + \mathbf{b}_0^{(1)} \right) \\ &+ \epsilon^2 \left(\sum \mathcal{G}_{ab} \mathbf{M}_a \mathbf{M}_b \mathbf{b}_0^{(0)} + \sum \mathcal{G}_a \mathbf{M}_a \mathbf{b}_0^{(1)} + \mathbf{b}_0^{(2)} \right) \\ &+ \epsilon^3 \left(\sum \mathcal{G}_{abc} \mathbf{M}_a \mathbf{M}_b \mathbf{M}_c \mathbf{b}_0^{(0)} + \sum \mathcal{G}_{ab} \mathbf{M}_a \mathbf{M}_b \mathbf{b}_0^{(1)} + \sum \mathcal{G}_a \mathbf{M}_a \mathbf{b}_0^{(2)} + \mathbf{b}_0^{(3)} \right) \\ &+ \epsilon^4 \left(\sum \mathcal{G}_{abcd} \mathbf{M}_a \mathbf{M}_b \mathbf{M}_c \mathbf{M}_d \mathbf{b}_0^{(0)} + \sum \mathcal{G}_{abc} \mathbf{M}_a \mathbf{M}_b \mathbf{M}_c \mathbf{b}_0^{(1)} \right. \\ &\left. + \sum \mathcal{G}_{ab} \mathbf{M}_a \mathbf{M}_b \mathbf{b}_0^{(2)} + \sum \mathcal{G}_a \mathbf{M}_a \mathbf{b}_0^{(3)} + \mathbf{b}_0^{(4)} \right) + \dots \end{aligned}$$

$$\mathcal{G}_{ab\dots} := \mathcal{G}(\ell_a, \ell_b, \dots; x)$$

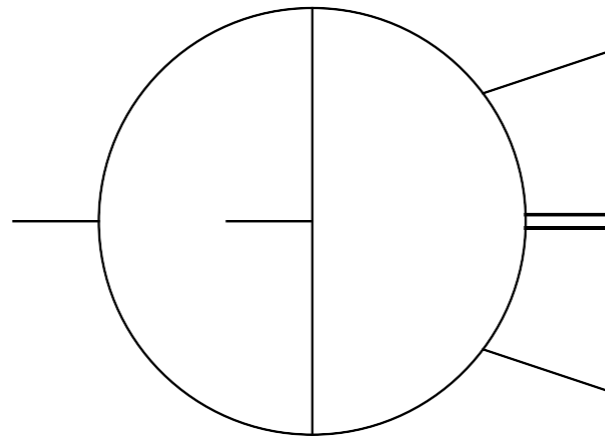
High Energy Physics Phenomenology and Computational Physics

Two-loop integrals: non-planar case

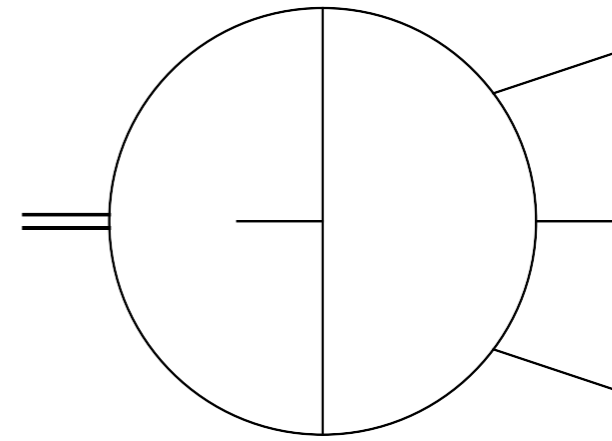
[JHEP 05 \(2022\) 033](#)



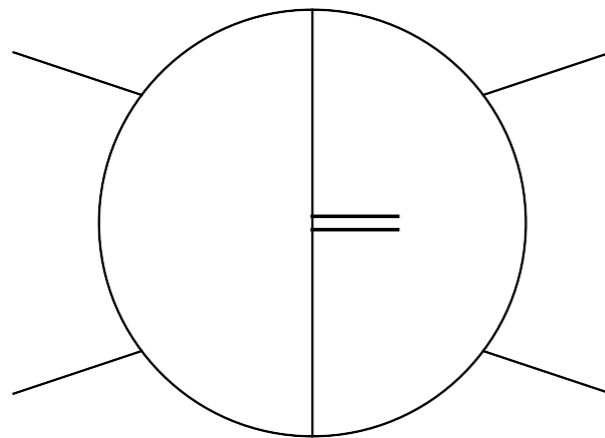
86,3



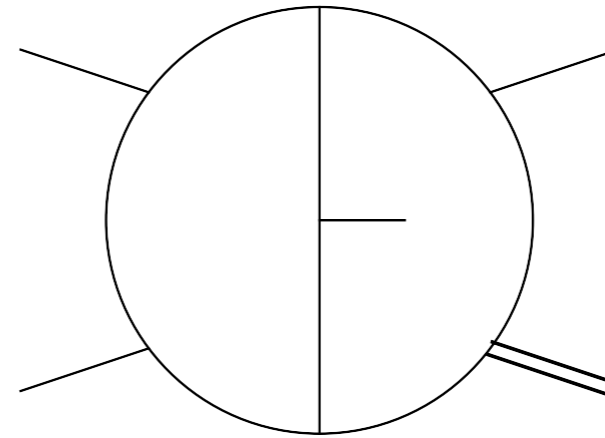
86,3



135,3



179,9



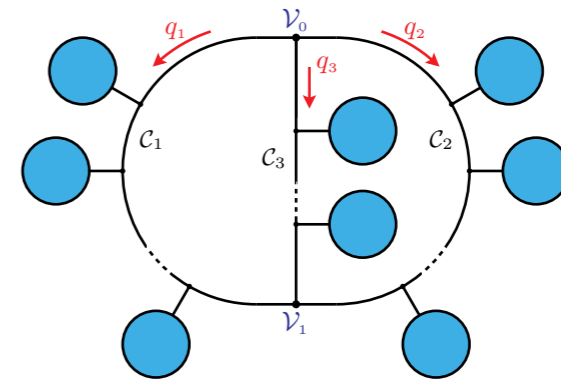
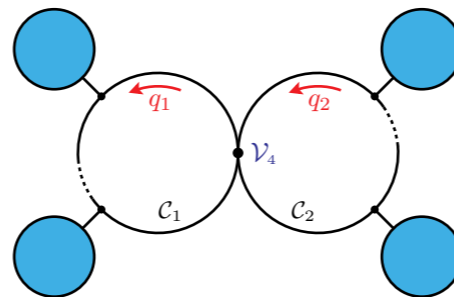
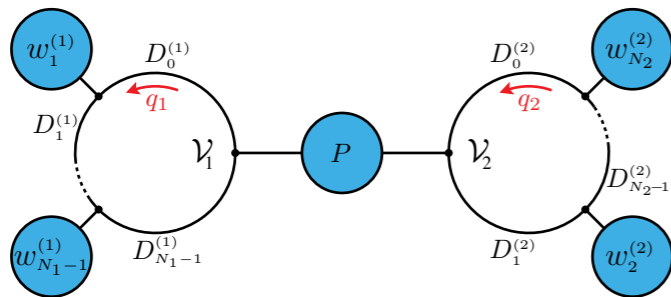
142,9

one-loop pentagon and three-loop planar

[JHEP 06 \(2021\), 037](#)

[JHEP 02 \(2021\), 080](#)

High Energy Physics Phenomenology and Computational Physics



$$A^{(L)} = \sum_{\Gamma \in \Delta} \sum_{i \in I_{\Gamma}} c_{\Gamma,i} \mathcal{M}_{\Gamma,i}$$

$$A^{(L)} = \sum_{\Gamma \in \Delta} \sum_{k \in N_{\Gamma}} \tilde{c}_{\Gamma,k} \frac{m_{\Gamma,k}(\ell)}{\prod_{j \in P_{\Gamma}} D_j}$$

$$\int \left(\prod \frac{d^d \ell_a}{(2\pi)^d} \right) \frac{m_{\Gamma,k}(\ell)}{\prod_{j \in P_{\Gamma}} D_j} = \begin{cases} \mathcal{M}_{\Gamma,k} & k \in M_{\Gamma} \\ 0 & k \in S_{\Gamma} \end{cases}$$

High Energy Physics Phenomenology and Computational Physics

Snowmass 2021 white paper

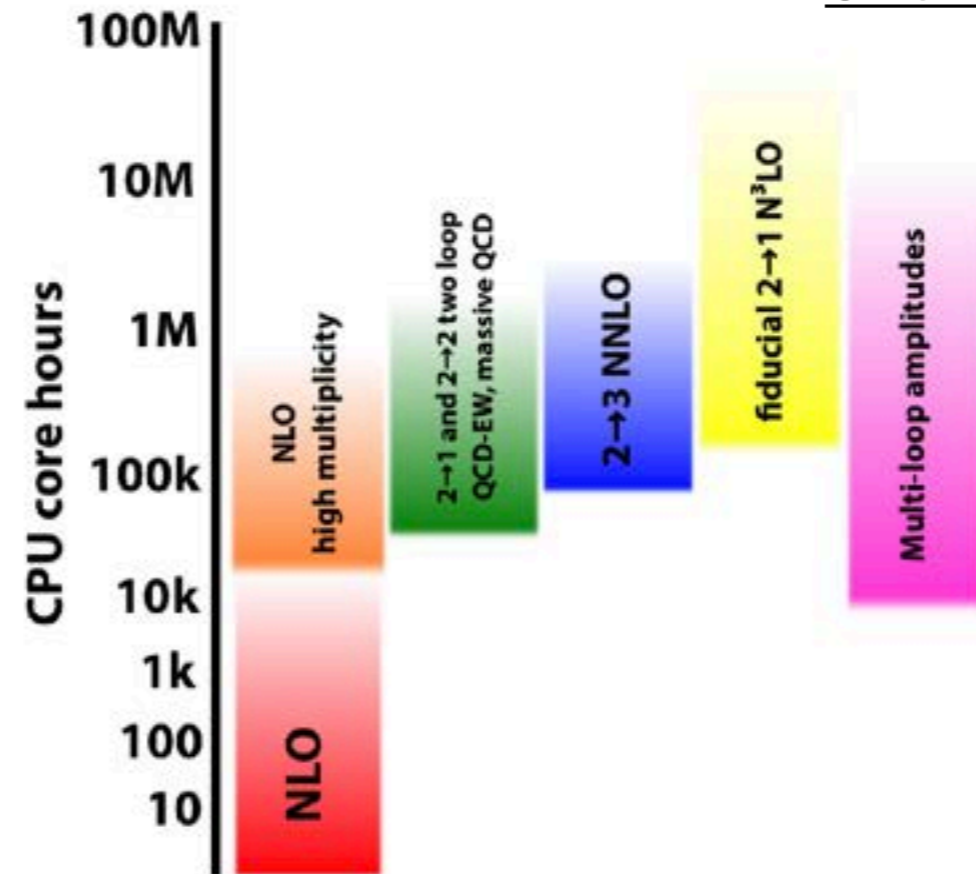
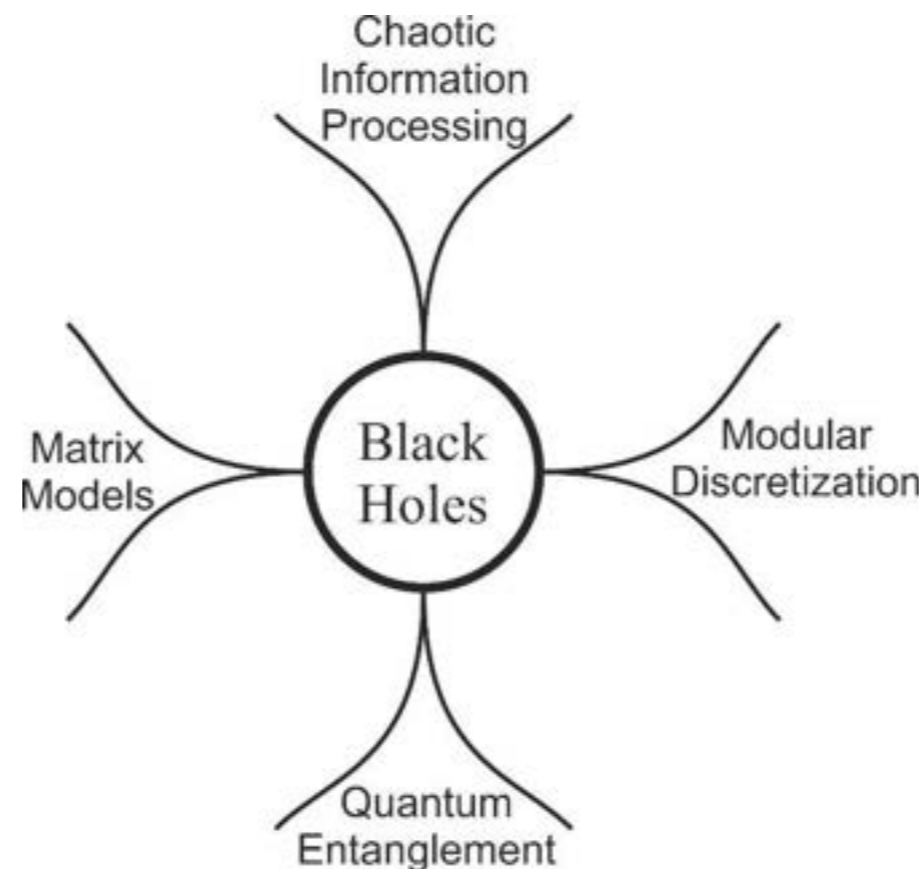


Figure 1: Run-time requirements of recent perturbative calculations for collider phenomenology. Memory requirements ranged up to about 2 TB of RAM per node.

THEORETICAL HIGH ENERGY PHYSICS GROUP

Our Research target is : Study of classical and quantum properties of space-time horizons (BHs, AdS)

Our Research demonstrates : Quantum BHs are “Cross-Fertilizers” of Information theory, Geometry ,
Chaotic Dynamics and Number theory

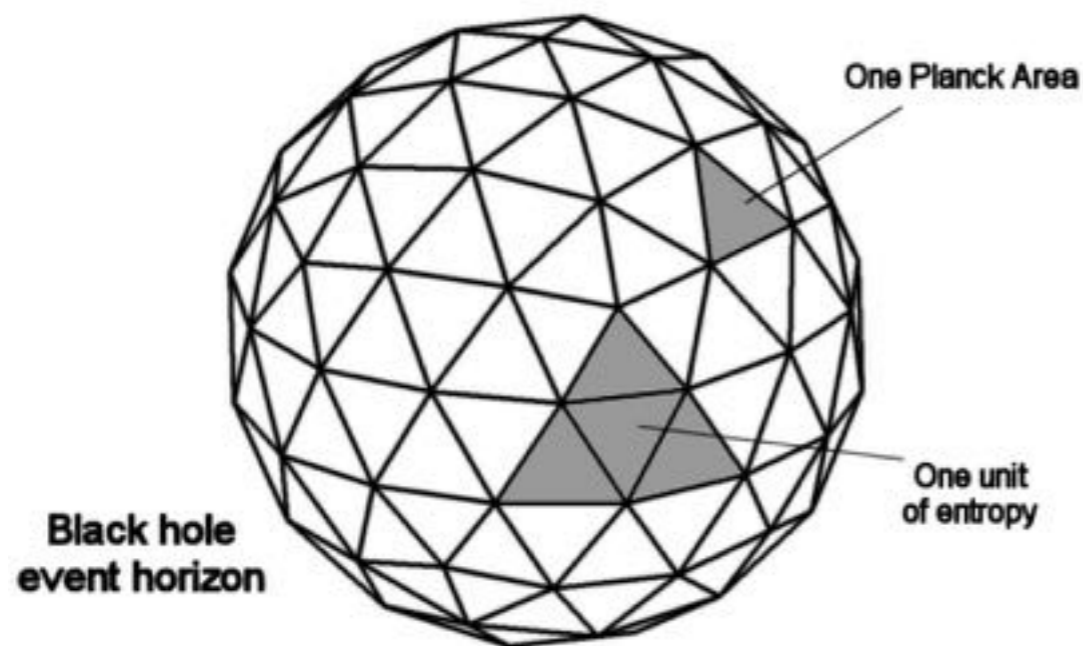


THEORETICAL HIGH ENERGY PHYSICS GROUP

IT FROM QUBIT

Black Hole Horizons possess: Finite # of microscopic d.o.f with a Finite dimensional Hilbert Space of States

Holographic Bekenstein-Hawking finite quantum entropy

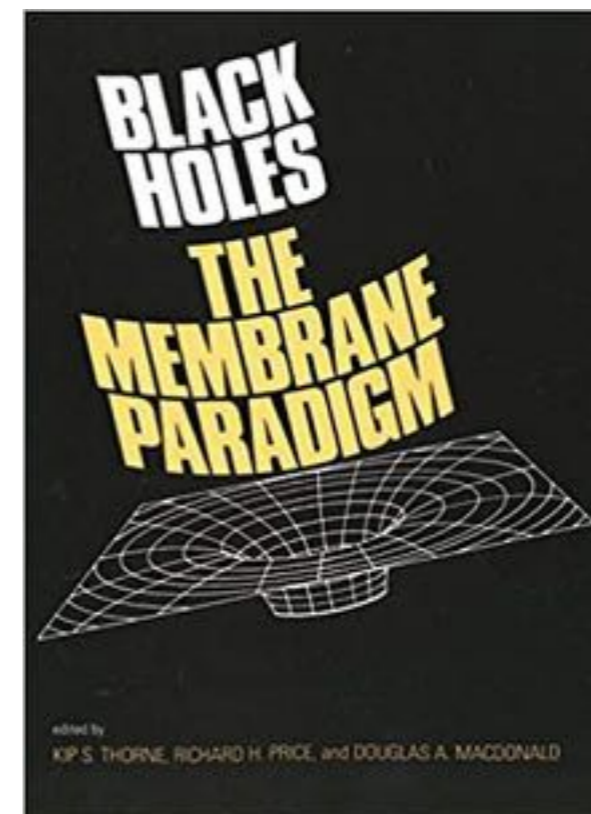
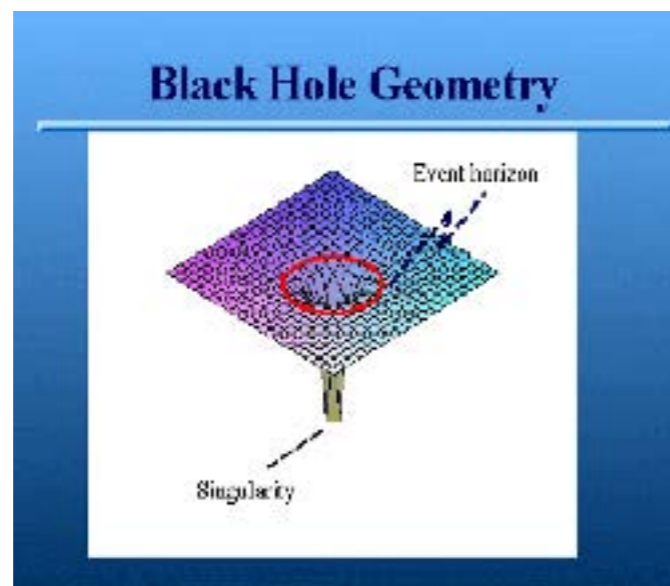


$$S_{BH} = \frac{c^3 A}{4G\hbar} \stackrel{n.u.}{=} \frac{A}{4}$$

THEORETICAL HIGH ENERGY PHYSICS GROUP

Black Hole Near Horizon Geometry : A stretched space-time at Planck length distance (10^{-33} cm) from the Event Horizon

- BH-horizon is a classically radiating **surface (membrane)** electrically charged with conducting properties, finite entropy and temperature.
- Our Work incorporates higher dimensional Berenstein-Maldacena-Nastase(BMN)-Matrix Model effects demonstrating Non-locality and Chaos

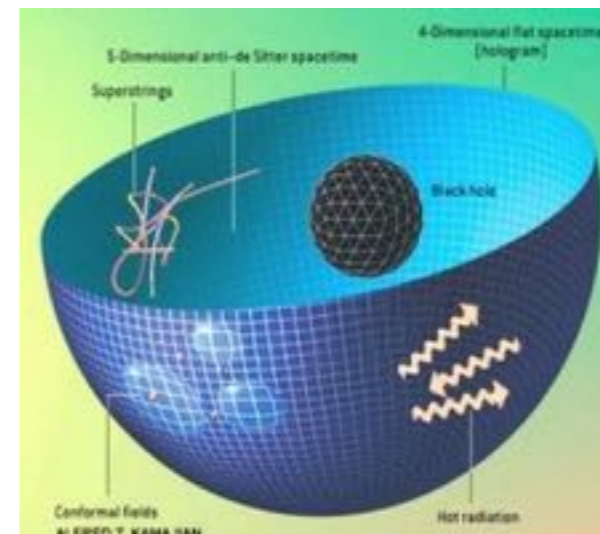
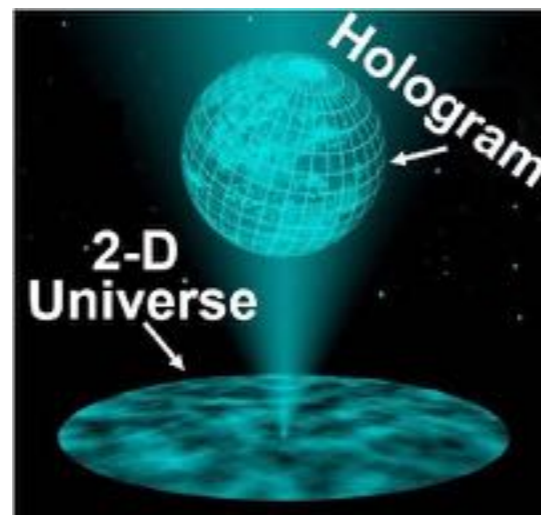


THEORETICAL HIGH ENERGY PHYSICS GROUP

NECESSARY: Theoretical Ingredients for modelling Unitary Quantum Information Processing by BH
(Sekino-Susskind, Heyden-Preskill, Shenker-Stanford, Maldacena et.al..)

1. Non locality (Beyond Field theories)
2. Strong Chaotic and random dynamics
3. Superfast scrambling of incoming Information
4. Entanglement between the outgoing and incoming particles must carry away the “lost information” saving unitarity.

We work within the framework of the Holographic Principle ('t hooft-Susskind) +AdS/CFT(Maldacena) :
INFORMATION OF A VOLUME IS ENCODED ON ITS SURFACE BOUNDARY



Project 1. “Quantum Entanglement in Many Body Quantum Systems and Black Holes”.

<http://happen.inp.demokritos.gr> (holographic applications of quantum entanglement)

16 Publications in Int.Journals & 5 Conference Proceedings

Eur.Phys.J.C 78 (2018) 4, 282 JHEP 02 (2020) 091 Phys.Rev.D 101 (2020) 8, 086015 JHEP 09 (2019) 106

Eur.Phys.J.C 78 (2018) 8, 668 JHEP 05 (2021) 203 Phys.Lett.B 781 (2018) 238-243 JHEP 11 (2020) 128

- Entanglement Entropy & Mutual Information in Many Body Systems, Scalar Fields (Srednicki’s Area Law), Entanglement Thermodynamics.
- Minimal Surfaces and the Ryu-Takayanagi Conjecture in AdS/CFT.
- Development of Methodology (Dressing Method, Polmeyer Reduction in NLSMs) for obtaining classical string solutions in specific Geometries.
- AdS/dCFT (G. Linardopoulos): 4 publications + 1 conference proceedings.
- ➔ **2019 Academy of Athens: “Lykourgeion Prize in Theoretical Physics”**



Future Plans: (M.Axenides with M. Floratos, S. Nicolis and G. Linardopoulos)

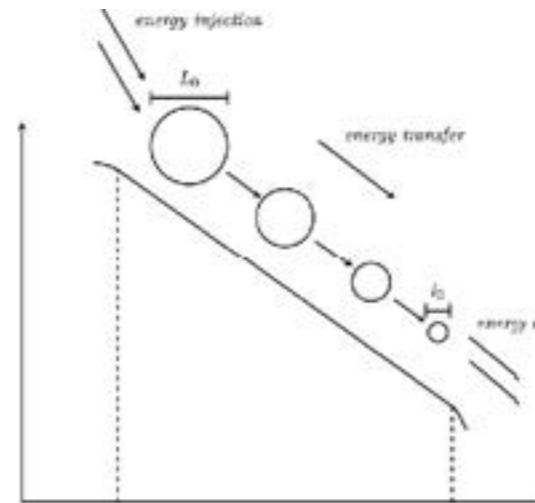
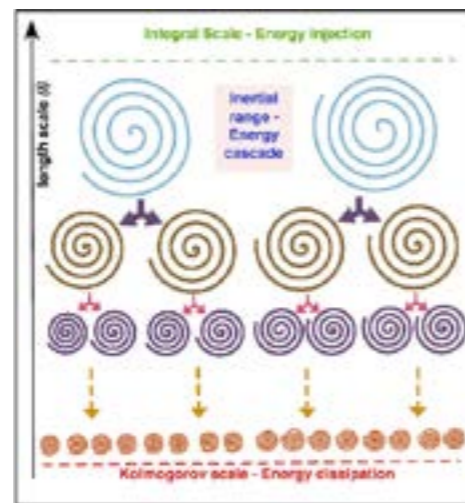
- Further develop exact methods in the computation of Entanglement Entropy and Mutual Information in Quantum Many body Systems as well as their Entanglement Thermodynamics.
- Study of all aspects of Quantum Entanglement in :
1. Many body Chaotic Quantum Systems with Non Local Interactions (e.g. Arnold Cat Map Lattices) and
 2. Quantum Chaotic Lattice Field Theory in general.

Project 2. “Chaos in the classical limit (Membrane) of the (Berenstein-Maldacena-Nastase) Matrix Model in 11-d M-theory”.

Researchers : M.Axenides, G.Linardopoulos, E.G. Floratos and D.Katsinis(Ph.D)

3 Publications in Int.Journals & 1 Conference Proceedings

- Strong Chaotic Instabilities are observed in a detailed higher order angular perturbative analysis of a classical $SO(3)$ closed membrane with flux obeying a cascade pattern:
 - **dipole $j=0$, and quadruple $j=1$** perturbations are unstable to lowest order in the perturbative stability analysis with all the rest stable.
 - They induce a cascade of instabilities for all j multipole 2nd order perturbations.(Smoking gun for weak turbulence ?)
- Future Plans: **IDENTIFY POSSIBLE** KOLMOGOROV TYPE ENERGY SCALING IN MEMBRANE INSTABILITY CASCADES



[Phys.Rev.D 104 \(2021\) 10, 106002](#)

[Phys.Rev.D 97 \(2018\) 12, 126019](#)

[Phys.Lett.B 773 \(2017\) 265-270](#)

Project 3. “Finite (Arithmetic) Quantum Mechanics ”.

1. Planck Scale Space-Time Modelling
2. Arithmetic Quantum Computation

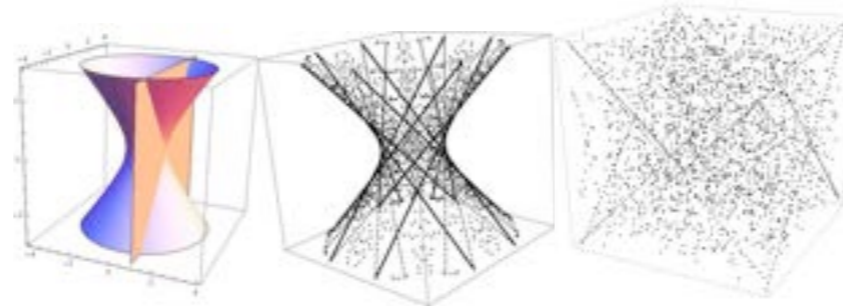
Researchers : M.Axenides, G.Linardopoulos, E.G. Floratos and A.Pavlidis

4 Publications in Int.Journals & 2 Conference Proceedings

An Arithmetic Geometry Model Proposal for Planck Scale Space-time Near Horizon Black Hole Geometry

e.g. **AdS(2,R) ≡ Near Horizon Geometry of Extremal BHs**

$$\text{AdS}(2,R) \rightarrow \text{AdS}(2,Z) \rightarrow \text{AdS}(2, Z/Z_n)$$



SIGMA 17 (2021) 004

Eur.Phys.J.C 78 (2018) 5, 412

JHEP 02 (2014) 109

Modular Arithmetic Discretisation exhibits:

- Non-Locality and Strong Chaos for single particle Probe Dynamics
- Finite Hilbert Space of States for Black Hole Horizon microscopic degrees of freedom
- Fast Scrambling and Propagation for Quantum information

Goals:

- **Formulation** of Classical and Quantum Chaotic Many-body Lattices & Field theories. (Arnold’s Cat Map Lattices)
- **Formulation** of Arithmetic Quantum Circuits on paper and their possible development in the Lab (QI-QCT @INPP)

Integration of the MIXMAX Engine into the CERN Scientific Software for MC Simulations: CLHEP, Geant4, ROOT, PYTHIA

Parameters of the MIXMAX Generator

K. Savvidy and G. Savvidy

Dimension N	Entropy $h(T)$	Decorrelation Time $\tau_0 = \frac{1}{h(T)2N}$	Iteration Time t	Relaxation Time $\tau = \frac{1}{h(T) \ln \frac{1}{\delta v_0}}$	Period q $\log_{10}(q)$
8	220	0,00028	1	1,54	129
17	374	0,000079	1	1,92	294
240	8679	0,00000024	1	1,17	4389

Table 1: The MIXMAX parameters.

The MIXMAX is a genuine 61 bit generator on Galois field $GF[p]$,
Mersenne prime number $p = 2^{61} - 1$.

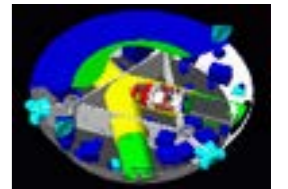
Unique high resolution generator: $\delta v_0 = 2^{-61N}$.

Most generators provide only $\delta v_0 = 2^{-32N}$ resolution.

A record generation time of 61 bit number is 4 nanosecond !

Development of the MIXMAX Random Numbers Generator:

1. The MIXMAX Consortium has developed a cutting-edge theory of the MIXMAX generator.
2. The MIXMAX code in C and C++ was developed by Konstantin Savvidis.
3. The MIXMAX code generates 64-bit high quality random sequences.
4. It is one of the fastest generators on the market.
5. <https://mixmax.hepforge.org>
6. <http://www.inp.demokritos.gr/~savvidy/mixmax.php>

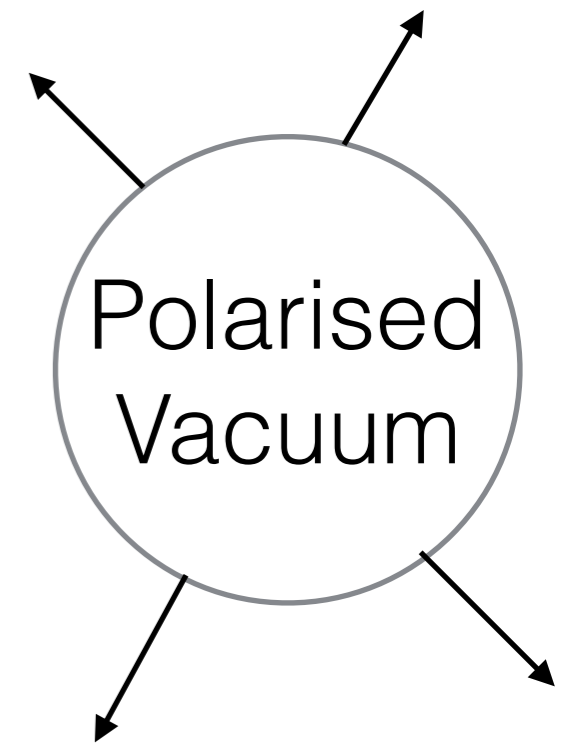


Worldwide acceptance of the open source MIXMAX Technology:

1. The MIXMAX generator has become the default option in **Geant4/CLHEP** software at CERN. Its areas of application include high energy, nuclear and accelerator physics, as well as studies in medical and space science:
<https://geant4.web.cern.ch> , <http://proj-clhep.web.cern.ch/proj-clhep/>
2. The MIXMAX generator has been offered as an addon in the **PYTHIA** software at Lund U
http://home.thep.lu.se/~torbjorn/doxygen/MixMax_8h_source.html
3. The MIXMAX generator is available for use with the **GSL - GNU Scientific Library**
<https://www.gnu.org/software/gsl/>
4. The MIXMAX generator is implemented in the **ROOT** library at CERN:
<https://root.cern.ch/doc/master/classTRandom.html>



*What is the Influence of the
Polarisation of the Vacuum
on Dark Energy and Cosmological Evolution?*



Y. B. Zel'dovich, *The Cosmological constant and the theory of elementary particles*,
Sov. Phys. Usp. **11** (1968) 381

S. Weinberg, *The Cosmological constant problem*, Rev. Mod. Phys. **61** (1989) 1-23

V. Mukhanov, *Physical Foundations of Cosmology*, Cambridge University Press, New York, 2005.

The vacuum energy density

$$E_0 = \int \frac{d^3p}{(2\pi)^3} \frac{1}{2} \omega_p \sim \frac{1}{16\pi^2} \Lambda^4 \quad \approx 1.44 \times 10^{110} \frac{g}{s^2 cm}$$

The contribution of zero-point energy exceed by many orders of magnitude the observational cosmological upper bound on the energy density of the universe

$$\epsilon_{crit} = 3 \frac{c^4}{8\pi G} \left(\frac{H_0}{c} \right)^2 \approx 7.67 \times 10^{-9} \frac{g}{s^2 cm}$$

$$\epsilon_\Lambda = 3 \frac{c^4}{8\pi G} \left(\frac{H_0}{c} \right)^2 \Omega_\Lambda \approx 5.28 \times 10^{-9} \frac{g}{s^2 cm}$$

Polarisation of the YM Vacuum and the Effective Lagrangians

$$\epsilon_{YM} = 3 \frac{c^4}{8\pi G} \frac{1}{L^2}, \quad \frac{1}{L^2} = \frac{8\pi G}{3c^4} \frac{11N - 2N_f}{196\pi^2} \Lambda_{YM}^4$$

Λ_{YM}^4 is the dimensional transmutation scale of YM theory

$$\epsilon_{YM} = 3 \frac{c^4}{8\pi G} \frac{1}{L^2} = \begin{cases} 9.31 \times 10^{-3} & eV \\ 9.31 \times 10^{29} & QCD \\ 9.31 \times 10^{97} & GUT \\ 9.31 \times 10^{110} & Planck \end{cases} \frac{g}{s^2 cm}$$

The YM vacuum energy density is well defined and is finite

The YM energy density is time depend function

Contribution of Vacuum Fluctuations

Heisenberg-Euler and Yang-Mills Effective Lagrangians

George Savvidy 1976

$$\left. \frac{\partial \mathcal{L}}{\partial \mathcal{F}} \right|_{t=\frac{1}{2} \ln\left(\frac{2e^2 |\mathcal{F}|}{\mu^4}\right)=\mathcal{G}=0} = -1, \quad ($$

where $\mathcal{F} = \frac{1}{4} G_{\mu\nu}^a G_{\mu\nu}^a$ is the Lorentz and gauge invariant form of the YM field strength tensor

Lamb shift - 1947

Casimir effect 1948

$$U_\gamma^\infty = \sum \frac{1}{2} \hbar \omega_k e^{-\gamma \omega_k}$$

$$\lim_{\gamma \rightarrow 0} [U_\gamma^\infty(J) - U_\gamma^\infty(0)] = U_{phys}$$

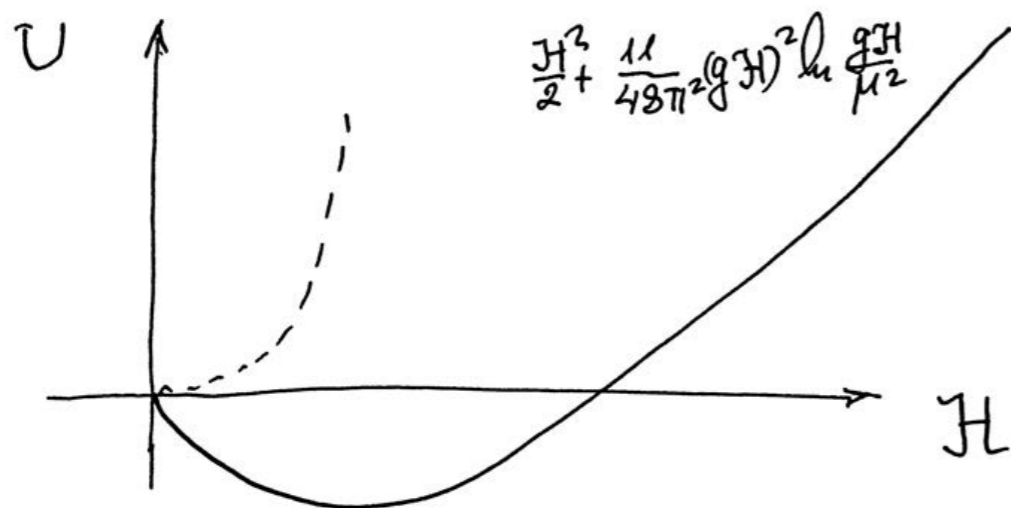
Dimensional Transmutation and Condensation

George Savvidy 1977, 2020

$$\mathcal{L}_g = -\mathcal{F} - \frac{11N}{96\pi^2} g^2 \mathcal{F} \left(\ln \frac{2g^2 \mathcal{F}}{\mu^4} - 1 \right),$$

$$\mathcal{F} = \frac{\vec{\mathcal{H}}_a^2 - \vec{\mathcal{E}}_a^2}{2} > 0, \quad \mathcal{G} = \vec{\mathcal{E}}_a \vec{\mathcal{H}}_a = 0.$$

$$\mathcal{L}_q = -\mathcal{F} + \frac{N_f}{48\pi^2} g^2 \mathcal{F} \left[\ln \left(\frac{2g^2 \mathcal{F}}{\mu^4} \right) - 1 \right]$$



$$2g^2 \mathcal{F}_{vac} = \mu^4 \exp \left(-\frac{96\pi^2}{b g^2(\mu)} \right) = \Lambda_{YM}^4,$$

where $b = 11N - 2N_f$.

Quantum Energy Momentum Tensor

$$T_{\mu\nu} = T_{\mu\nu}^{YM} \left[1 + \frac{b g^2}{96\pi^2} \ln \frac{2g^2 \mathcal{F}}{\mu^4} \right] - g_{\mu\nu} \frac{b g^2}{96\pi^2} \mathcal{F}, \quad \mathcal{G} = 0,$$

$$T_{00} \equiv \epsilon(\mathcal{F}) = \mathcal{F} + \frac{b g^2}{96\pi^2} \mathcal{F} \left(\ln \frac{2g^2 \mathcal{F}}{\mu^4} - 1 \right) \quad T_{ij} = \delta_{ij} \left[\frac{1}{3} \mathcal{F} + \frac{1}{3} \frac{b g^2}{96\pi^2} \mathcal{F} \left(\ln \frac{2g^2 \mathcal{F}}{\mu^4} + 3 \right) \right] = \delta_{ij} p(\mathcal{F}).$$

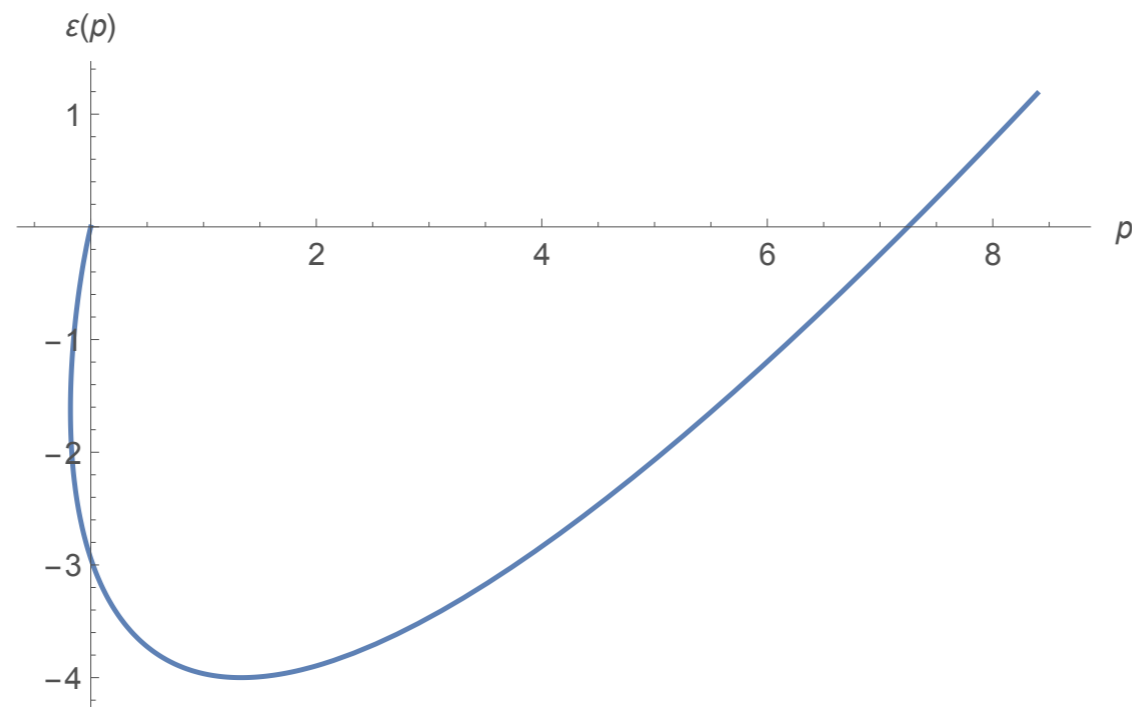
$$\epsilon(\mathcal{F}) = \mathcal{F} + \frac{b g^2}{96\pi^2} \mathcal{F} \left(\ln \frac{2g^2 \mathcal{F}}{\mu^4} - 1 \right),$$

$$p(\mathcal{F}) = \frac{1}{3} \mathcal{F} + \frac{1}{3} \frac{b g^2}{96\pi^2} \mathcal{F} \left(\ln \frac{2g^2 \mathcal{F}}{\mu^4} + 3 \right).$$

$$\mathcal{F} = \frac{1}{4} g^{\alpha\beta} g^{\gamma\delta} G_{\alpha\gamma}^a G_{\beta\delta} \geq 0$$

$$\mathcal{G} = G_{\mu\nu}^* G^{\mu\nu} = 0$$

Yang-Mills Quantum Equation of State



$$\epsilon(\mathcal{F}) = \mathcal{F} + \frac{b g^2}{96\pi^2} \mathcal{F} \left(\ln \frac{2g^2 \mathcal{F}}{\mu^4} - 1 \right), \quad p(\mathcal{F}) = \frac{1}{3} \mathcal{F} + \frac{1}{3} \frac{b g^2}{96\pi^2} \mathcal{F} \left(\ln \frac{2g^2 \mathcal{F}}{\mu^4} + 3 \right).$$

general parametrisation of the equation of state $p = w\epsilon$

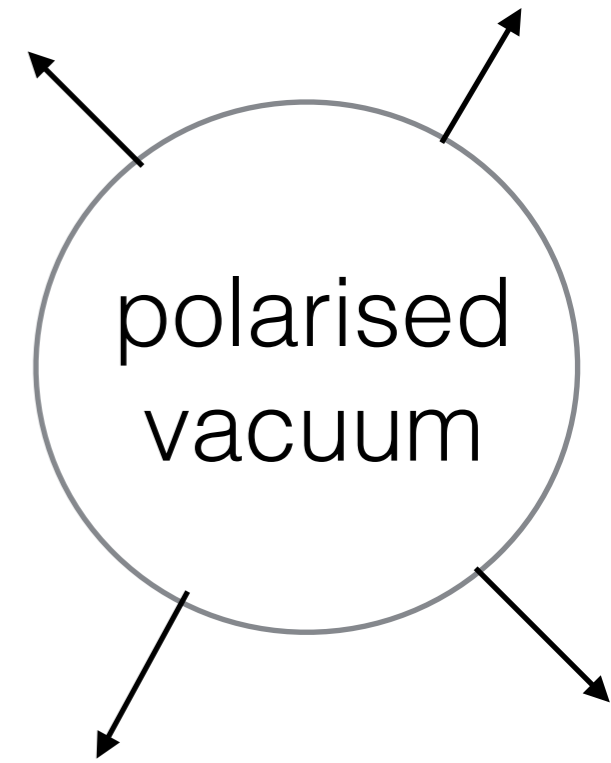
$$p = \frac{1}{3}\epsilon + \frac{4}{3} \frac{b g^2 \mathcal{F}}{96\pi^2} \Lambda_{YM}^4 \quad \text{and} \quad w = \frac{p}{\epsilon} = \frac{\ln \frac{2g^2 \mathcal{F}}{\Lambda_{YM}^4} + 3}{3 \left(\ln \frac{2g^2 \mathcal{F}}{\Lambda_{YM}^4} - 1 \right)}$$

GR Action

$$S = -\frac{c^3}{16\pi G} \int R \sqrt{-g} d^4x + \int (\mathcal{L}_q + \mathcal{L}_g) \sqrt{-g} d^4x.$$

$$R_{\mu\nu} - \frac{1}{2}g_{\mu\nu}R = \frac{8\pi G}{c^4} \left[T_{\mu\nu}^{YM} \left(1 + \frac{b g^2}{96\pi^2} \ln \frac{2g^2 \mathcal{F}}{\mu^4} \right) - g_{\mu\nu} \frac{b g^2}{96\pi^2} \mathcal{F} \right].$$

$$\Lambda_{eff} = \frac{8\pi G}{c^4} \epsilon_{vac} = -\frac{8\pi G}{c^4} \frac{b}{192\pi^2} 2g^2 \mathcal{F}_{vac} = -\frac{8\pi G}{c^4} \frac{b}{192\pi^2} \Lambda_{YM}^4$$



The YM field strength \mathcal{F} is not a constant function of time but evolve in time in accordance with the Friedmann equations, thus the cosmological term here is time dependent

- The Type I-IV solutions of the Friedmann equations induced by the gauge field theory vacuum polarisation provide an alternative inflationary mechanism and a possibility for late-time acceleration.
- The Type II solution of the Friedmann equations generates the initial exponential expansion of the universe of finite duration and the Type IV solution demonstrates late time acceleration.
- The solutions fulfil the necessary conditions for the amplification of primordial gravitational waves.

Topics for PhD thesis

1. Gauge Field Theory Vacuum and Cosmological Inflation
2. Maximally Chaotic Dynamical Systems and Fundamental Interactions
3. Accretion disks, Emission in Active Galactic Nuclei, Jets and Accretion Disks

4. Reduction at the integrand level beyond one loop
5. HELCA2L development
6. Simplified Differential Equations approach for massive Feynman Integrals

7. Many-body Arnold's cat-map dynamics: Classical and Quantum Properties, Information and Thermodynamic aspects

Topics for MSc thesis

1. Gauge Field Theory Vacuum and Cosmological Inflation
2. Maximally Chaotic Dynamical Systems and Fundamental Interactions
3. Accretion disks, Emission in Active Galactic Nuclei, Jets and Accretion Disks

4. Simplified Differential Equations approach
5. HELCA1L development

Thank you for your attention